Effect of turbine section orientation on the performance characteristics of an oscillating water column device

Sandeep K. Patel, Krishnil Ram and M. Rafiuddin Ahmed*
Division of Mechanical Engineering, The University of the South Pacific, Suva, Fiji

Abstract

Oscillating water column (OWC) devices are the most successful devices for extracting energy from ocean waves. In oscillating water column devices, the air turbine section is of either horizontal or vertical orientation. An experimental study is carried out to compare the airflow characteristics and turbine rpm in horizontal and vertical turbine sections of an oscillating water column device. Two OWC models, one with a horizontal duct connecting the turbine to the atmosphere and the other with a vertical duct, were tested at mean water depths of 230 mm, 260 mm and 290 mm and at frequencies of 0.6 Hz, 0.7 Hz, 0.8 Hz, 0.9 Hz, 1.0 Hz and 1.1 Hz. Mean total pressure profiles were plotted just upstream and downstream of the turbine section for different cases, while instantaneous static and dynamic pressure measurements were performed to study their variations with time at these locations. A Savonius type rotor was used as a turbine and its rpm was measured and at the above depths and frequencies to compare the performance of the two OWC models. The OWC model with the horizontal turbine section showed better performance characteristics compared to the OWC with the vertical turbine section. RPM values were 20 - 30% greater in the horizontal turbine orientation compared to the vertical one. The successful use of a Savonius type rotor as a good and cost-effective option for energy conversion is emphasized in this work.

Keywords: Oscillating water column, Savonius rotor, Wave energy converter, Pressure measurements.

1. Introduction

Increasing global energy consumption is now well-known to have serious environmental implications and recent years have seen a drive to produce energy from renewable sources. A promising source of renewable energy is from the ocean waves and interest in developing machines to convert energy from waves is steadily increasing. Wave energy is generally considered to provide a clean source of renewable energy, with limited environmental impacts which could contribute significantly to the reduction of greenhouse gases produced by conventional fossil fuels [1]. The magnitude of the incident wave energy, along 30,000 km of Pacific Ocean coasts, has been estimated to be around 1013 kWh per year. This value approximates to the world electric energy consumption registered in the year 2000 [2]. Not only is the wave energy resource vast, it is also more dependable than most renewable energy resources [3,4]. In order to exploit the benefits of such a renewable energy source, a wide variety of devices, based on different energy-extracting methods, have been proposed [4] but only a few are actually installed [5,6]. The greatest challenges to designers of wave energy converters are the intrinsically oscillating nature and the random distribution of the wave energy resource [7]. The response of a wave energy device is generally frequency dependent. The peak (resonant) frequency and a range of frequencies that will produce a significant response will depend on the particular device [1]. The most successful and most extensively studied device for extracting energy from the ocean waves is the oscillating water column (OWC) device [8]. There are a number of companies that have commercialized this technology following pilot installations around the globe including Portugal, Scotland, Japan and Australia. The OWC wave energy converter (WEC) comprises a partly submerged structure open below the water surface, inside which air is trapped above the free water surface [9]. Approaching waves force the internal free surface of the water to oscillate; this causes an oscillation of the pressure of the air in the chamber and forces an air flux forwards and

backwards through an air turbine, installed in a duct which connects the chamber to the atmosphere [8].

Oscillating water column (OWC) devices are divided into two main categories; fixed-type OWC and the floating-type OWC devices. In OWCs, the air turbine is either vertical (Toftstalen, Norway, 1985; Trivandrum, India, 1990) or of horizontal axis (Pico, Portugal, 1999; Limpet, UK, 2000; Port Kembla, Australia, 2005) [9]. The bi-directional airflow is unique to this device and requires the use of a bi-directional turbine. There are several such turbines including Wells turbine, impulse turbines and Savonius type turbines. The Wells turbine was the first choice for all the OWC based wave energy plants which were built in Norway, Japan, Scotland, India and China. A Wells turbine is a self-rectifying air turbine which rotates in a single direction and extracts mechanical shaft power from such bi-directional air flow as in case of an OWC device [10]. There are many reports which describe the performance of the Wells turbine both at starting and running conditions. According to these results, however, the Wells turbine has inherent disadvantages in comparison with conventional turbines: lower efficiency and poorer starting characteristic [11]. The efficiency of OWC devices equipped with Wells turbines is particularly affected by the flow oscillations basically for two reasons: first, because of the intrinsically unsteady (reciprocating) flow of air displaced by the oscillating water free surface; second, because increasing the air flow rate above a limit and approximately proportional to the rotational speed of the turbine, is known to give rise to a rapid drop in the aerodynamic efficiency and in the power output of this turbine [12].

Of late, there is a growing interest in rectangular OWC chambers and rectangular turbine sections housing Savonius rotors [13,14]. A design of a Savonius rotor utilizing OWC is presented by Dorrell et al. [13-15]. They compared multiple chamber arrangements and reported conversion rates of 20.2% for the two bladed Savonius turbine. The advantage lies in the simplicity of design

and the ease of construction of these types of turbines as well as the OWC. It also allows increasing of the width of OWC parallel to the coast so that a greater amount of energy can be absorbed per device. Unlike the circular OWC, the width of entry of the capture chamber can be increased in the rectangular ducted OWC without being influenced by the diameter at the turbine section [16]. The Savonius turbine is a much effective solution at low Reynolds numbers, unlike the Wells turbine which requires a high Reynolds number [13].

Menet [17] remarked that Savonius rotors are simple machines and their high starting torque enables them not only to run, but also to start at whatever the air velocity. The components which convert the mechanical energy into electrical energy can be placed at the surface which makes maintenance operations simple. It cannot be ignored that Savonius rotors have lower efficiencies than horizontal axis turbines for wind applications. However in the case of OWCs, the simplicity of the Savonius rotor along with its other advantages makes it a competitive option for power take-off. This is a simple and low-cost turbine although the conversion factor is low [18]. The design and construction of such a turbine is simpler and does not require complex understanding of aerodynamics and blade design. Hence it is also suitable for private installations by communities or individuals for small systems. Similar to VAWTs, this turbine can be constructed easily with readily available tools and material as compared to the other wave energy turbines which require complex design and specialized equipment to construct. In 2008, Altan and Atılgan [19] proposed the idea of a curtain placed in front of a Savonius wind rotor to increase its aerodynamic performance. The curtain causes air to be channeled onto the inner blades rather than impacting the outer portion of the adjacent blade; this reduces negative torque on the Savonius rotor. The contracting curtains need to be placed on both sides of the turbine due to the bi-directional flow. A novel way of incorporating the curtain effect into the chamber of the OWC is employed in the present work.

The design presented in the present work uses a capture chamber structure that can be incorporated into a breakwater to reduce structural costs. The Savonius rotor is simpler and cheaper [17] to construct and this leads to cost reduction of the turbine system. Use of a Savonius type rotor allows the rotor shaft to run perpendicular to the airflow. This allows the shaft to be extended out of the OWC chamber, so that the generation unit is mounted outside for easy access for maintenance. The present work is aimed at experimentally studying the airflow characteristics and Savonius rotor rpm in two OWC devices with vertical and horizontal turbine sections.

2. Experimental method

The experiments were carried out in a Cussons wave channel, model P6325, available in the Thermo-fluids Laboratory of the University of the South Pacific. The wave channel is 3500 mm long, 300 mm wide and 450 mm deep. The side walls are made of Plexiglas to allow a clear view of the wave action. This wave channel uses a flap type wave-maker hinged at the bottom to generate sinusoidal waves. The close fit of the wave-maker to the channel sides ensures that 2-D waves are produced with no fluid motion normal to the sidewalls [20]. The water flow is generated by a centrifugal pump having a rated capacity of 40 Lit/s at a total head of 10 m and is driven by a 5.5 kW motor. The pump draws water from a tank, as shown in Fig. 1. Different sea conditions (wave height, wave length etc.) can be simulated in the wave channel by changing the frequency of the wave-maker. Some of the wave characteristics are presented in ref. [21]. Fig. 1 shows a schematic diagram of the wave channel.

A Cussons Tuneable Beach, model P6285, was placed at the other end of the wave channel. The tuneable beach uses a series of porous plates (large holes to small size holes) mounted in the path of the waves. Each porous plate is designed with a pattern of holes to absorb some wave energy, allow the rest to pass through the plate, and minimize reflection. The use of different

plates with a variable spacing between them allowed a wide variety of wave profiles to be absorbed.

Two OWC models were built out of clear Perspex, one with a horizontal turbine section and the other with a vertical turbine section. Figure 2 shows the OWC model with the horizontal turbine section and Fig. 3 shows the OWC model with vertical turbine section. The models were built to a scale of 1:100. Koola et al. used a scale of 1:100 and stated that in Froude scale, the model ratio is proportional to the square of the time ratio [22]. An acceptable range of Froude scaling is 60-150 [in ref. 22]. Both the models have the same dimensions for the capture chamber and the turbine section including the inlet and the outlet of the turbine section. The diffusers at the exit of the turbine section, which serve as nozzles when the airflow is from the atmosphere, also have exactly the same dimensions. The rear wall of the OWC models is inclined at 65° to reduce wave reflections. The angle was determined after a comparison of different capture chamber angles. Since majority of the water particles in shallow water have horizontal trajectories the inclination aids in aligning the near horizontal velocities to the capture chamber to avoid reflection. The detailed methodology and results of identifying the optimum angle is presented in [23]. Selecting an inclined water column in shallow shoreline conditions also offers and easier path for water to ingress and egress resulting in less turbulence and lower energy loss [**24**]. The design has a rectangular capture chamber and a turbine section to allow the use of a Savonius type rotor as the turbine. A similar rectangular ducted OWC for Savonius type rotor was designed and tested by Ram et al. [21]. The nozzle serves two important purposes: one is to increase the velocity of air flowing towards the turbine section and the other is to direct the flow of air to allow maximum impact of air striking the Savonius rotor blades [16,21].

The total pressure was measured across the cross-section at pressure taps 5 and 8 shown in Figs. 2 and 3 and the profiles of the mean total pressure were plotted for different cases. A total

of 10 pressure taps were provided on the surface starting from the inclined surface right through to the diffuser for measuring the static pressure. Flexible tubes were connected to the pressure taps and a Furness Controls, FCO510 model, digital micro-manometer, transferred the static and dynamic pressure data to a PC. The measurements of the pressures were normally limited to the first 10-15 second after switching on the wave-maker; this was done to ensure that the reflections from the OWC model do not affect the measurements. An S-type probe, fabricated and calibrated in-house, was inserted at the pressure taps 5 and 8. The same digital micro-manometer was also used to measure the differential pressure from the S-type probe. The differential pressure provided the dynamic pressure values at tap 5 and tap 8. The dynamic pressure fluctuations were used to study the instantaneous velocity trend at these locations. The airflow characteristics were studied at the depths (D) of 230 mm, 260 mm and 290 mm and frequencies (f) of 0.6 Hz to 1.1 Hz with increments of 0.1 Hz for the two OWC models with horizontal and vertical turbine sections. A five bladed Savonius type rotor was designed and constructed in the lab. The rotor has a length of 190 mm and a diameter of 65 mm, as shown in Fig. 4. The blades of the Savonius rotor are made of Aluminum and are curved at an angle of 70°. The shaft is a mild steel rod of diameter 3 mm. The accuracy of pressure measurements with FCO510 micromanometer is 0.01 mm of water. The repeatability of the pressure measurements was within 3.2%. The accuracy of the digital tachometer, used for measuring the rpm of the Savonius rotor is 2.8%. The repeatability of rpm measurements was within 2.6%. Torque measurements were not possible with reasonable accuracy as the rotors did not develop enough power to surpass the inertia of torque sensors.

3. Results and discussion

3.1. Total pressure across the air column cross-section

The results of the measurements of total pressure across the cross-section at tap 5 and tap 8 for different cases are presented in this section. The pressure taps 5 and 8 are located at the same distance from the center of the turbine section. The distance 'h' is measured from the rear wall and non-dimensionalized with respect to the distance between the walls, H. The total pressure was non-dimenionalized against the incident wave height (H_w) to define the air pressure ratio. The air pressure ratio is a parameter used to compare the performance of various types of pneumatic wave power devices **[25]**.

Figure 5 shows the total pressure distributions at tap 5 for outward flow and tap 8 for inward flow, before the air enters the turbine, for the horizontal section case for f = 1.0 Hz and D = 260 mm. The total pressure at tap 5 indicates the total pressure of the air that is exhaled in the inlet nozzle when the water level inside the chamber rises as a result of wave impingement. The total pressure at tap 8 indicates the total pressure of air sucked from the atmosphere in the nozzle connecting the turbine section to the atmosphere during the inward flow as the water level inside the chamber falls when the wave recedes. The total pressure at the inlet during outward flow is higher than the total pressure at the inlet during inward flow. This is because of the exhalation of the air that is already trapped inside the OWC chamber when the water level rises, resulting in a higher pressure. These high total pressures, which, at pressure tap 5 are due to a higher static pressure and a lower dynamic pressure translate into a lower static pressure and a higher dynamic pressure at the section where the area is less, and will be discussed later. On the other hand, the total pressure at the inlet to the turbine, at pressure tap 8, is lower because during the inward flow, the air from the atmosphere is sucked inside the OWC chamber which results in a lower total pressure. It can also be seen the total pressure distribution is quite uniform across the cross-section of the chamber except at the points close to the rear wall, despite the fact that the flow changes its orientation from the inclined chamber to the horizontal turbine section.

It was found that the airflow velocities and the rotor rpm are the highest for f = 1.0 Hz and D = 260 mm for both horizontal and vertical orientations of the turbine section. For this reason, detailed measurements of pressures were performed for this case.

Figure 6 shows the total pressure distributions at tap 5 and tap 8 for the OWC with the horizontal turbine section for f = 1.0 Hz and D = 260 mm. The total pressure at inlet was measured at tap 5 and that at the outlet was measured at tap 8. The difference between the two indicates the total pressure loss between the two stations. It has been reported in the past [26] that the air jet coming from the atmosphere into the chamber during the downward motion of the internal water surface impinges directly onto the free-surface pulverizing the water. The resulting water droplets are subsequently transported during the outward airflow. According to Sarmento et al. [26], this has two effects – it reduces the turbine rotational speed and erodes the turbine blades. However, their observation was based on a Wells turbine, while in the present case, a Savonius rotor is employed. The transported water droplets increase the density of the air and since the Savonius rotor works purely on momentum transfer, they may not have a significant influence on the rotational speed of the turbine. Paixao Conde and Gato [9] proposed the use of a baffle plate beneath the turbine's duct to inhibit the production of water spray at the water free surface.

Figure 7 shows the total pressure distributions at taps 5 and 8 for the OWC with the vertical turbine section at f = 1.0 Hz and D = 260 mm. The total pressure at inlet, which is at the bottom, is considerably higher than the total pressure at the exit, which is at the top, indicating a much higher total pressure loss compared to the horizontal turbine case. It should be noted that the entire outward flow in the vertical turbine OWC system is against gravity. On top of that, during the outward flow, the density of the air is higher due to the presence of water droplets. In spite of this, the total pressure at tap 5 during the outward flow is always higher than the total pressure at

tap 8 during the inward flow, due to the compression of the trapped air, as discussed earlier. At the outlet (tap 8), the total pressure is higher at the middle of the duct than near the walls.

There is also a possibility that the vertical duct is handling a higher quantity of the denser air (air with water droplets) because of the gravity effect, compared to the horizontal duct which will loose some of the dense air as it leaves the OWC device and draws some fresh lower density air during the inward flow.

3.2. Wall static pressures

The results of the static pressure measurements for both the OWC models are presented in this section. Figure 8 shows the static pressure fluctuations for both the OWC models at the water depth of 260 mm and the frequency of 1.0 Hz, recorded for duration of 10 seconds after starting the wave-maker. At this depth and frequency, the turbine rpm was the highest for both the OWC models, as mentioned earlier. It can be seen that static pressures are higher for the OWC model with the vertical turbine section compared to the OWC model with horizontal turbine section. This higher value of static pressures for the OWC model with vertical turbine section indicates lower velocity and the lower value of static pressures for the OWC model with horizontal turbine section indicates higher velocity. It is also interesting to observe that the negative pressures during the inward flow have higher negative values compared to the positive pressures during the outward flow. Similar observations were made by Krishnil Ram et al. [21]. At the exit of the turbine i.e. at tap 8, the static pressures reduce, as shown in Fig. 9, as the total pressure reduces across the turbine. The reduction is higher for the OWC model with vertical turbine section. At the same time, the static pressure values are higher for the vertical case, indicating lower velocities compared to the horizontal case.

3.3. Dynamic Pressures

The results of the dynamic pressure measurements for both the OWC models are analyzed and presented in this section. Figure 10 shows the dynamic pressure fluctuations for both the OWC models at the mean water depth of 260 mm and the frequency of 1.0 Hz, recorded at tap 5. It can be seen that dynamic pressures are higher for the OWC model with horizontal turbine section compared to the OWC model with vertical turbine section. The higher values of dynamic pressures simply mean higher velocity or higher energy available to the turbine. It is interesting to observe that the positive values are much higher compared to the negative values. Similar trends are reported by Sarmento et al. [26], who reported considerably higher positive values of dynamic pressures compared to negative values. Paixao Conde and Gato [9] also reported that the positivie velocities during the outward flow are higher compared to the negative velocities during the inward flow. Similarly, higher air flow rates were reported by Brito-Melo et al. [27] during the outward flow compared to the inward flow.

At the pressure tap 8, the dynamic pressure values reduce significantly, as shown in Fig. 11. Further to the discussion on total pressure reduction (loss) between tap 5 and tap 8 for the vertical case, it can be seen from Fig. 11 that the dynamic pressure values for the vertical case are very small, which combined with small static pressures, result in a lower total pressure at tap 8. The values of dynamic pressure also reduce considerably from pressure tap 5 to tap 8 for the horizontal turbine section. The velocity of the air increases continuously from tap 2 to tap 5 due to a reduction in area (not shown) and then reduces across the turbine.

It is important to note that in both cases (vertical and horizontal), the turbine section is closer to the atmosphere. This is common in most OWC designs. This means that during the inhalation stage there is very little difference in the energy available to the turbine in both cases. While the vertical chamber may possess some advantage as the flow would be favored by gravity, the short

distance the air travels in duct to reach the turbine in both cases makes this insignificant. The exhalation stage can be considered to the governing factor as the air travels a significant distance to reach the turbine and is affected by the geometry of the turbine duct section. The capture chamber is of the same geometry in both cases as well. The exhalation stage velocities are usually greater that the inhalation stage in an OWC [9, 26, 27]. In the vertical duct, the flow is against gravity during exhalation and hence slowed down before imparting energy onto the turbine blades. During the horizontal case, the flow does not incur sustained climb against gravity as the duct becomes horizontal causing the flow to exit easily. Another factor that may play a role in enhancing the horizontal ducts performance is the nature of boundary layers in both cases. Flow in a horizontal duct would tend to discourage boundary layer growth. As the duct becomes horizontal, particles would still have some effect of gravity. Instead of having purely horizontal motion, the resultant motion of the particles would be inclined downwards owing to the addition of the forward motion and effect of gravity. This would ensure a greater velocity at closer to the bottom wall than that in the middle of the duct. This would discourage boundary layer growth on the bottom wall. The turbulence created by the bend would also re-energise the flow and reduce boundary layer growth. In the vertical duct the straight path of air against gravity causes boundary layers to develop on the walls. This may also add to the vertical sections poor performance. According to results, effects of the bend in the horizontal section is outweighed by the benefits of the horizontal section. In fact it has been reported by [28] that the losses due to a 90^{o} bend between the capture chamber and the air duct is negligible, less than 0.01%.

3.4. Rotational Speeds

The results of the measurements of rotational speed of both the OWC models are presented in this section. Table 1 shows the rpm of the Savonius rotor at different depths and frequencies for both the OWC models. It can be seen that at frequencies of 0.6 Hz and 0.7 Hz, the rotor does not rotate at all the three water depths of 230 mm, 260 mm and 290 mm. At these lower frequencies, low amplitude waves are generated, which do not generate enough air pressure to cause rotation of the rotor. High amplitude waves generated at higher frequencies cause larger oscillations inside the OWC column, considerably increasing the total pressure of the air which results in the rotation of the turbine. It can also be seen from Table 1 that there is higher energy extraction by the Savonius rotor when employed in the OWC model with horizontal turbine section compared to the OWC model with vertical turbine section at all the water depths and frequencies studied in the present work. As mentioned earlier, the highest values of rpm for both the OWC models were recorded at the mean water depth of 260 mm and the frequency of 1.0 Hz. At this depth and frequency, the rpm of the rotor in the horizontal section OWC is 19.4% greater than the vertical OWC. The table also shows that the greatest difference in rpm for the two orientations occurs at a depth of 230 mm and a frequency of 1.0 Hz. For this case, the horizontal section gives 48.8% higher rpm than the vertical section. The rpm of the Savonius rotor for this depth and different frequencies can be seen graphically in Fig. 12. At the frequencies of 0.6 Hz and 0.7 Hz, the rpm is zero for both the OWC models, as mentioned earlier. At the frequency of 0.8 Hz, the OWC model with horizontal turbine section has higher rpm than the OWC model with vertical turbine section. Similar difference in the performance of the rotor is observed for f = 1.0 Hz and 1.1 Hz. Interestingly, at the frequency of 0.9 Hz, the rpm was zero for both the turbine orientations. At this depth of 230 mm, the OWC model with horizontal turbine section has a significantly better performance compared to the OWC model with vertical turbine section.

Figure 13 shows the rpm of the Savonius rotor for both the OWC models at different frequencies at D = 260 mm. Even for this depth, the rotor does not rotate at the lower wave frequencies of 0.6 Hz and 0.7 Hz, because of the low amplitude waves. At the frequency of 0.8 Hz, the OWC model with horizontal turbine section has higher rpm than the OWC model with vertical turbine section. At the frequency of 0.9 Hz, the rotor rpm for the horizontal case is slightly higher compared to the vertical case. At the higher frequencies of 0.9 Hz, 1.0 Hz and 1.1 Hz, the rotor for the horizontal turbine section has higher rpm values and the device is performing better than the vertical turbine section case.

Figure 14 shows the rpm of the Savonius rotor for the two OWC models at different frequencies at D = 290 mm. Again, there is not enough energy transfer to the rotor at the lower wave frequencies of 0.6 Hz and 0.7 Hz, and the rpm is zero for both the OWC models. At frequency of 0.8 Hz, the OWC model with horizontal turbine section has higher rpm than the OWC model with vertical turbine section. Interestingly, at f = 0.9 Hz, the rotor rpm for both the turbine orientations is found to be higher compared to f = 0.8 Hz at this depth; a totally different behavior compared to lower depths. There is almost a linear increase in the rotor rpm with increasing frequency at this depth. For all the frequencies, the OWC model with horizontal turbine section has a higher rotor rpm than the OWC model with vertical turbine section.

4. Conclusions

Two OWC models, one with a horizontal turbine section and the other with a vertical turbine section, were tested in a wave channel to study the airflow characteristics in the air chamber leading to the turbine section of the device. A Savonius rotor was employed as the power take-off device. The mean total pressure at the turbine inlet was higher during outward flow than during the inward flow with the compression of the trapped air resulting in a higher pressure after wave impingement. The static pressures were higher for the OWC model with the vertical turbine

section indicating lower velocities compared to the horizontal case. The dynamic pressures were higher for the horizontal case. Both the static and dynamic pressures reduced across the turbine. The OWC model with the horizontal turbine section showed superior performance compared to the vertical case in terms of rpm for all depths and frequencies. While both models have the same capture chamber which is largely responsible for tuning, this study has focused on the turbine ducts. Taking the total pressure, static pressure, dynamic pressure and rpm into account, it can be seen that the OWC model with the horizontal turbine section performed better compared to the OWC model with the vertical turbine section.

References

[1] G.H. Smith, V. Venugopal, The effect of wave period filtering on wave power, Ocean Engineering, 34 (2007) 1120-1137

[2] S.M. Camporeale, P.D. Strippoli, G. Pascazio and M. Torresi, Accurate numerical simulation of a high solidity Wells turbine, Renewable Energy, (2007).

[3] R. Pelc, R.M. Fujita, Renewable energy from the ocean, Marine Policy, 26 (2002), 471-479.

[4] B. Drew, A.R. Plummer, M.N. Sahinkaya, A review of wave energy converter technology, Proceedings of IMechE: Part A, Journal of Power and Energy, Vol. 223 (2010), pp. 887-902.

[5] AF de O Falcao, First-generation wave power plant: current status and R&D requirements, Proceedings of International Conference on Offshore Mechanics and Arctic Engineering (OMAE 2003) held in Cancun, Mexico.

[6] A. Clement, P. McCullen, A. Falcao, A. Fiorentino, F. Gardner, K. Hammarlund, et al., Wave energy in Europe: current status and perspectives, Renewable and Sustainable Energy Reviews, 6 (2002) 405-431.

[7] A. Brito-Melo, L. M. C. Gato and A. J. N. A. Sarmento, Analysis of Wells turbine design parameters by numerical simulation of the OWC performance, Ocean Engineering, 29 (2002), 1463-1477.

[8] K. Graw, Scale 1:10 wave flume experiments on IIT oscillating water column wave energy device, ODEC, (1993), 26-27.

[9] J. M. Paixao Conde and L.M.C. Gato, Numerical study of the air-flow in an oscillating water column wave energy converter, Renewable energy, 33 (2008), 2637-2644 .

[10] S. Santhakumar, H. Maeda, M. Takao, T. Setoguchi, A review of impulse turbines for wave energy conversion, Renewable Energy, 23 (2001), 261-292.

[11] T. Setoguchi, Y. Kinoue, K.K.M. Takao, Wells turbine with end plates for wave energy conversion, Ocean Engineering, 34 (2007), 1790-1795.

[12] A.F. de O. Falcao, P.A.P. Justino, OWC wave energy devices with air flow control, Ocean Engineering, 26 (1999), 1275-1295.

[13] C.C. Lin, D.G. Dorrell, A small segmented oscillating water column using a Savonius rotor turbine, Proceedings of IEEE International Conference on Sustainable Energy Technologies (ICSET 2008) held in Singapore, 508-513.

[14] D.G. Dorrell, W. Fillet, Investigation of a small-scale segmented oscillating water column utilizing a Savonius rotor turbine, Proceedings of the International Conference on Energy and Environment (ICEE 2006) held in Selangor, Malaysia, 23-32.

[15] D.G. Dorrell, M.F. Hsieh, C.C. Lin, Investigation of a small-scale segmented oscillating water column utilizing a Savonius rotor turbine, IEEE Transactions on Industry Applications, 46 (2010) 2080-2088.

[16] S.K. Patel, K. Ram, M.R. Ahmed and Y.H. Lee, Performance studies on an oscillating water column employing a Savonius rotor, Science China Technological Sciences, 54 (2011).

[17] J.L. Menet, A double-step Savonius rotor for local production of electricity, Renewable Energy, 29 (2004) 1843-1862.

[18] M.C. Percival, P.S. Leung, P.K. Datta, The development of a vertical turbine for domestic electricity generation, Proceedings of European Wind Energy Conference held in London, UK, (2004) 1-10.

[19] B.D. Altan, M. Atilgan, The use of a curtain design to increase the performance level of a Savonius wind rotors, Renewable Energy, 35 (2010) 821-892.

[20] M. Rea, Wave tank and wavemaker design, in Ocean wave energy – current status and future perspectives, ed. João Cruz, Springer-Verlag, Berlin Heidelberg, Germany, (2008) pp. 147-159.

[21] K. Ram, M. Faizal, M.R. Ahmed, Y.H. Lee, Experimental studies on the flow characteristics in an oscillating water column device, Journal of Mechanical Science and Technology, 24 (2010) 2043-2050.

[22] P. M. Koola, M. Ravindran, P. A. A. Narayana, Model studies of oscillating water column wave-energy device, ASCE Journal of Energy Engineering, 121 (1995) 14-26.

[23] K. Ram, M.A. Zullah, M.R. Ahmed, Y.H. Lee, Experimental studies on the flow characteristics in an inclined bend-free OWC device with parallel walls, Paper No. O-Oc-1-6, in: Proceedings of 'Renewable Energy 2010' International Conference, Yokohama, Japan, June 27 – July 2, 2010.

[24] Arup Energy, The Carbon Trust – Marine Energy Challenge, Oscillating water column wave energy converter evaluation report. The Carbon Trust. 2005.

[25] M.E. McCormick , Y.C Kim , Utilization of ocean waves – wave to energy conversion, Proceedings of the ASCE Speciality Conference, Utilization of Ocean Waves, Scripps Institution of Oceanography, June 16-17, 1986.

[26] A.J.N.A. Sarmento, F. Neumann, A. Brito-Melo, Oscillating water column – Pico plant, in Ocean wave energy – current status and future perspectives, ed. João Cruz, Springer-Verlag, Berlin Heidelberg, Germany, (2008) pp. 342-350.

[27] A. Brito-Melo, F. Neumann, A.J.N.A. Sarmento, Full-scale data assessment in OWC Pico plant, Proc. 17th International Offshore and Polar Engineering Conference, Lisbon, Portugal, July 1-6, (2007), 447-454.

[28] A. Gareev Analysis of variable pitch air turbines for oscillating water column (OWC) wave energy converters, Doctor of Philosophy thesis, University of Wollongong. School of Mechanical, Materials and Mechatronic Engineering, University of Wollongong, (2011). http://ro.uow.edu.au/theses/3418

List of Figures:

List of tables:

Figure 1

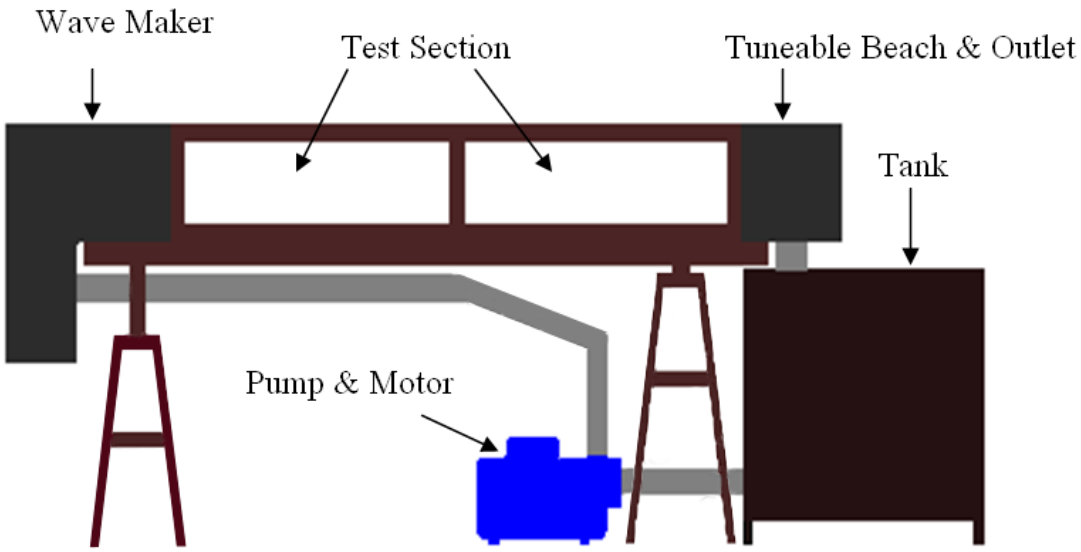

Fig. 1. Schematic diagram of the Wave Channel.

Figure 2

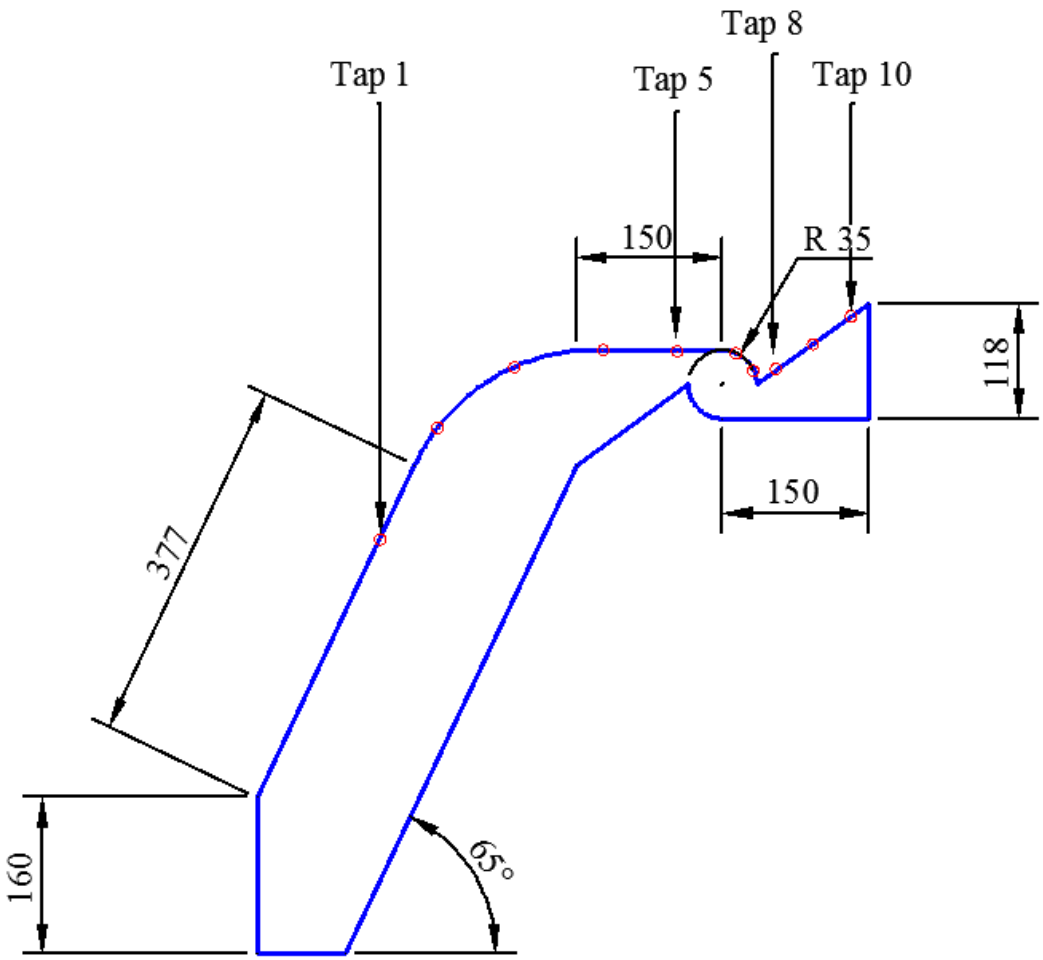

Fig. 2. Schematic diagram and geometric details of the OWC model with horizontal turbine section.

Figure 3

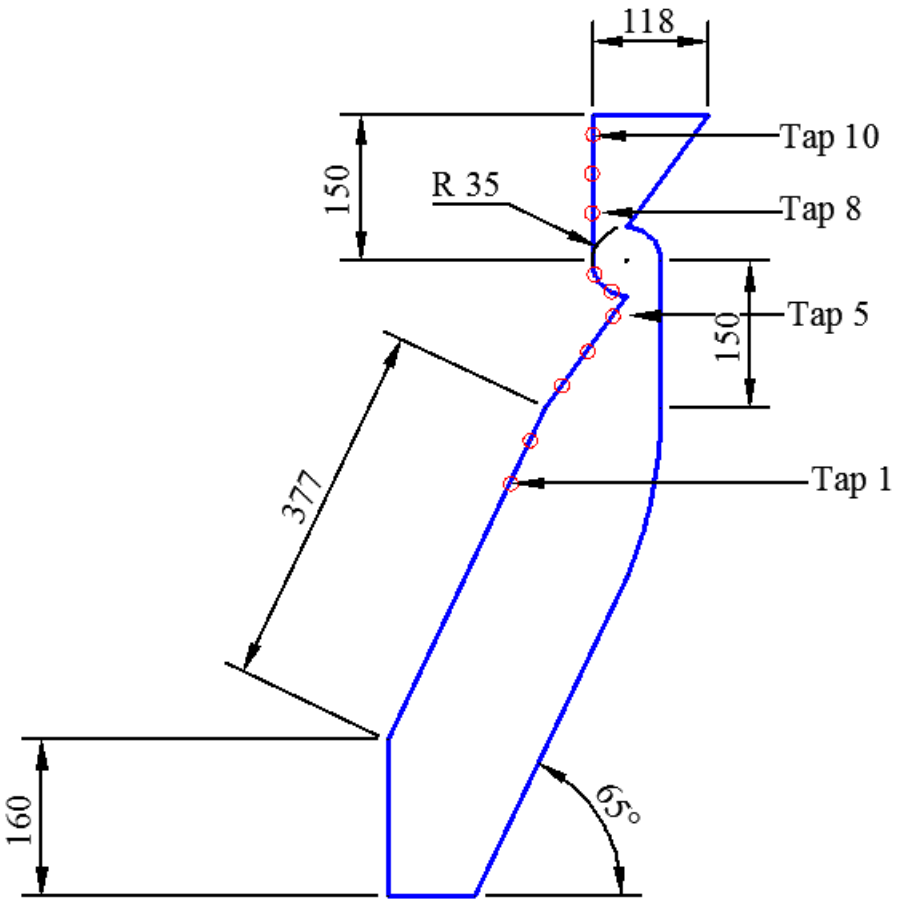

Fig. 3. Schematic diagram and geometric details of the OWC model with vertical turbine section.

Figure 4

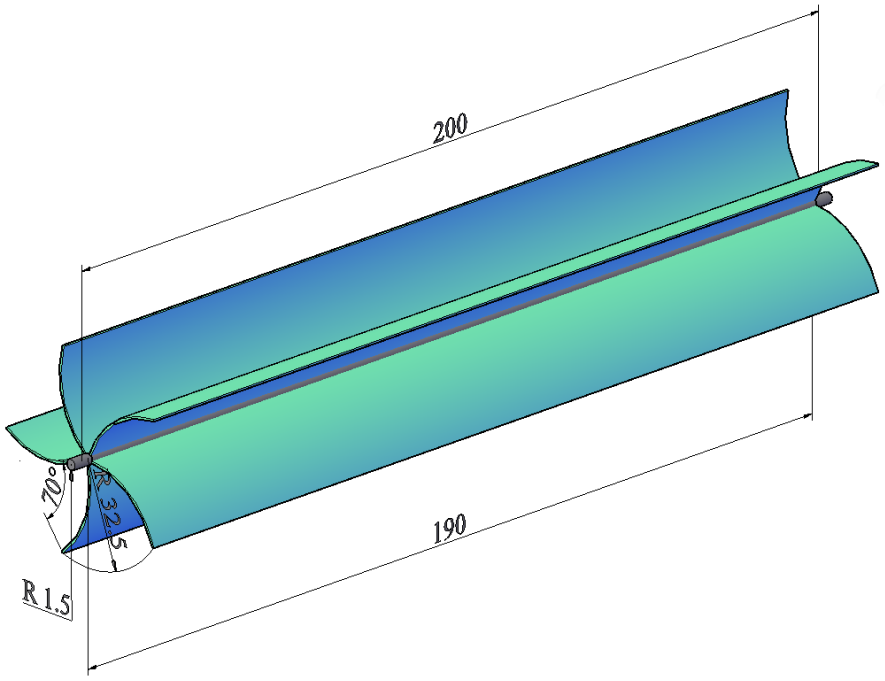

Fig. 4. Geometric details of the Savonius rotor.

Figure 5

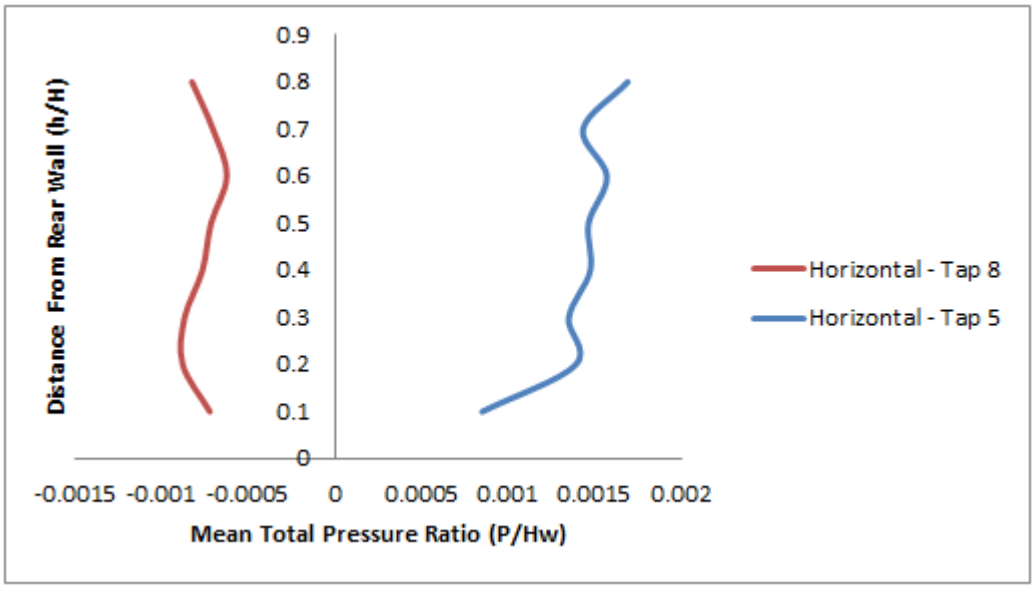

Fig. 5. Comparison of the total pressure distributions at the inlet to the turbine during outward and inward flows for the OWC model with horizontal turbine section at f = 1.0 Hz and D = 260 mm.

Figure 6

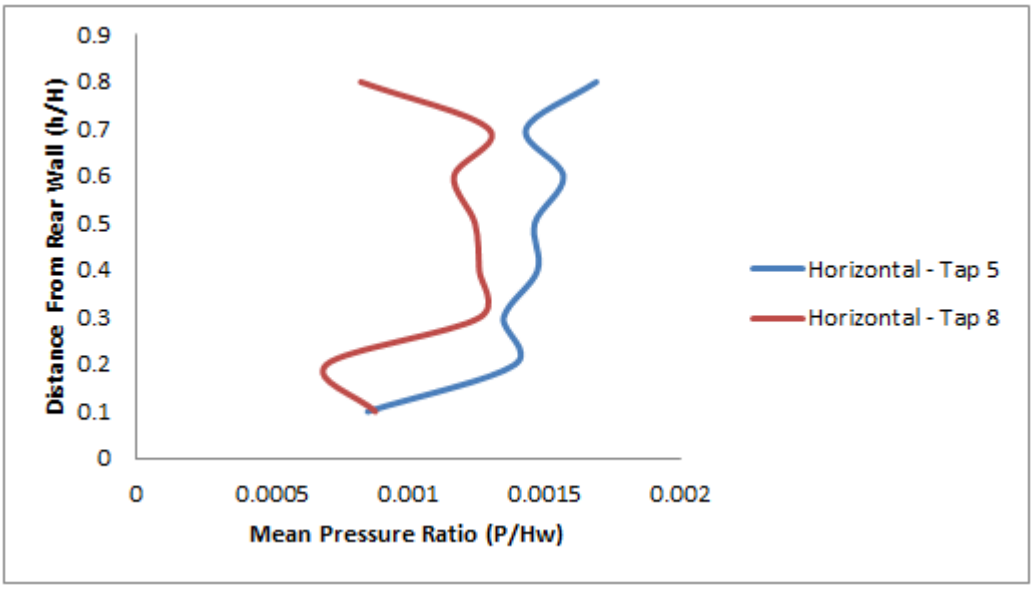

Fig. 6. Total pressure distributions at the inlet and exit of the turbine during outward flow for the OWC model with horizontal turbine section at f = 1.0 Hz and D = 260 mm.

Figure 7

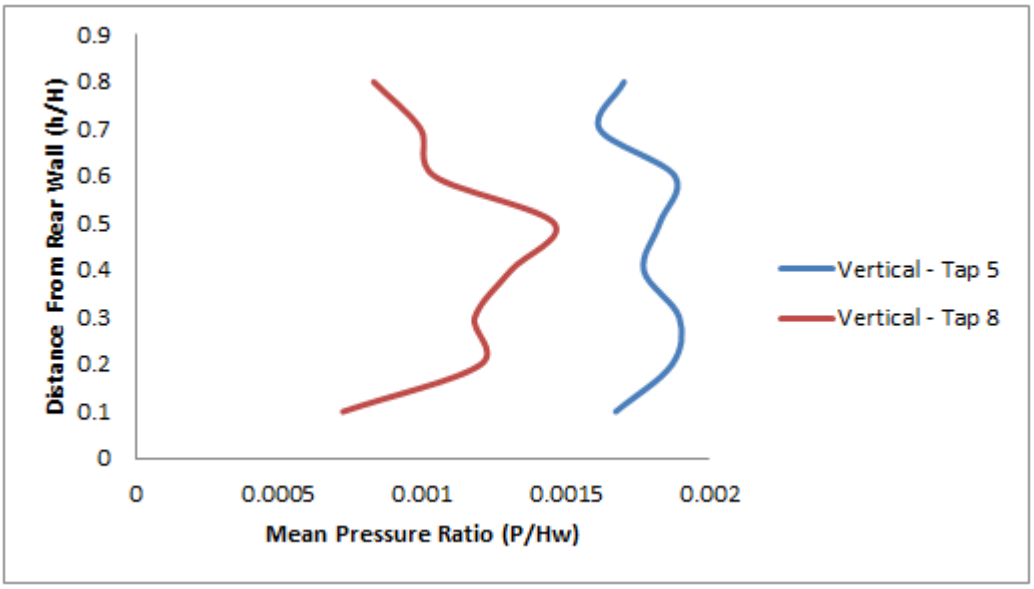

Fig. 7. Total pressure distributions at the inlet and exit of the turbine during outward flow for the OWC model with vertical turbine section at f = 1.0 Hz and D = 260 mm.

Figure 8

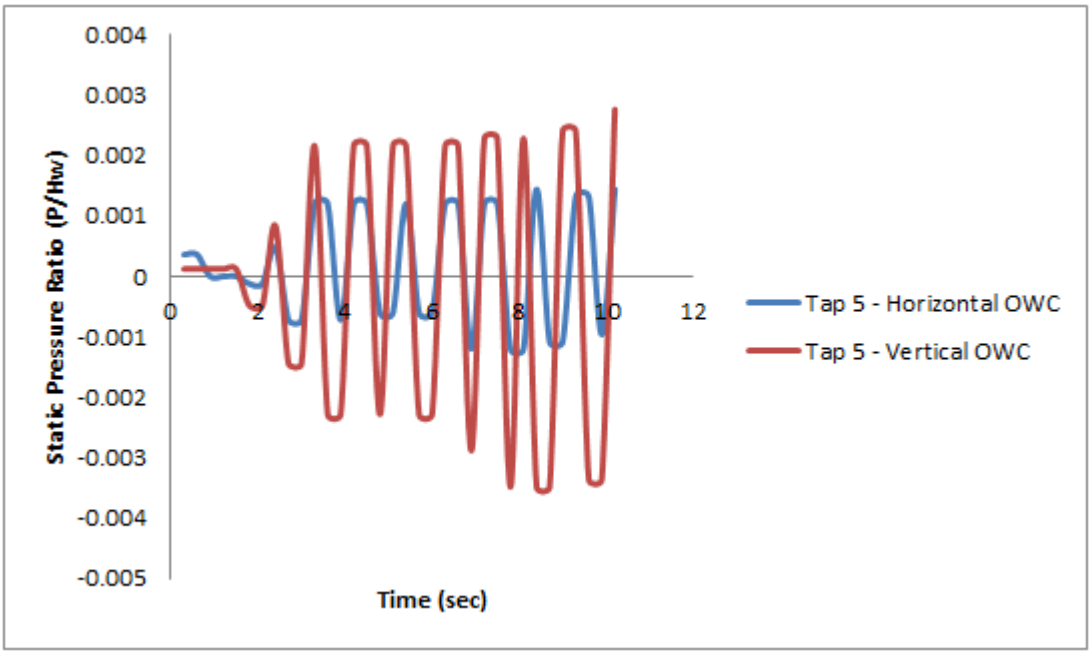

Fig. 8. Fluctuations in the static pressure at tap 5 for the two OWC models at f = 1.0 Hz and D = 260 mm.

Figure 9

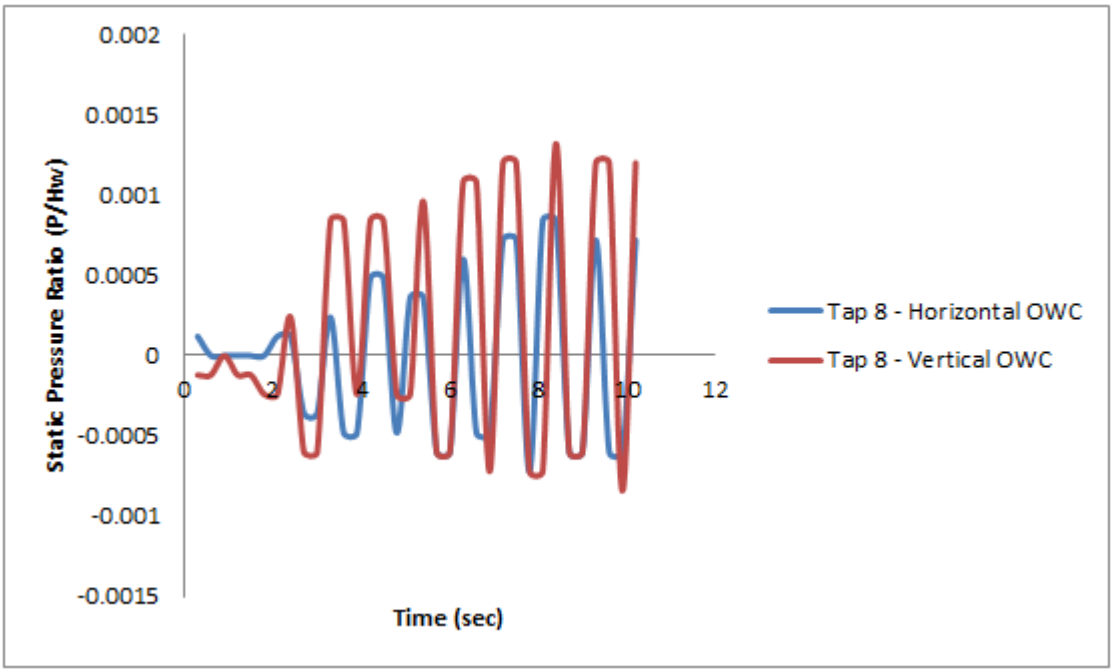

Fig. 9. Fluctuations in the static pressure at tap 8 for the two horizontal OWC models at f = 1.0 Hz and D = 260 mm.

Figure 10

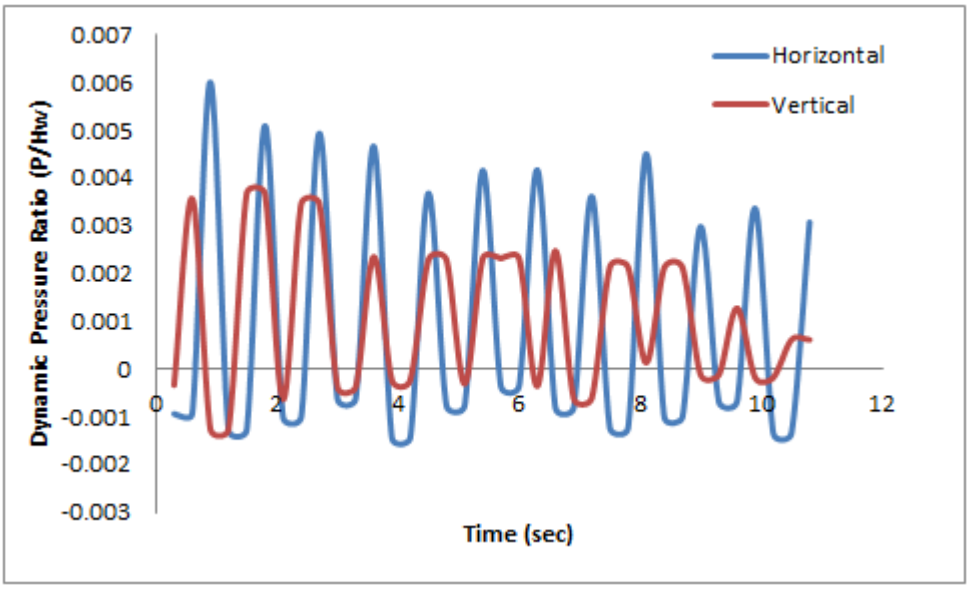

Fig. 10. Fluctuations in the dynamic pressure at tap 5 for the two OWC models at f = 1.0 Hz and D = 260 mm.

Figure 11

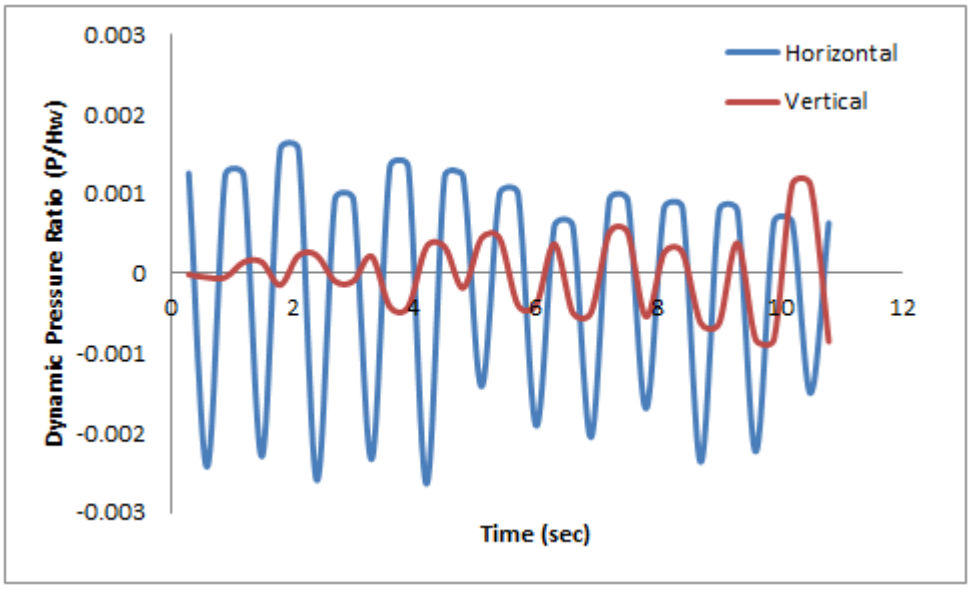

Fig. 11. Fluctuations in the dynamic pressure at tap 8 for the two OWC models at f = 1.0 Hz and D = 260 mm.

Figure 12

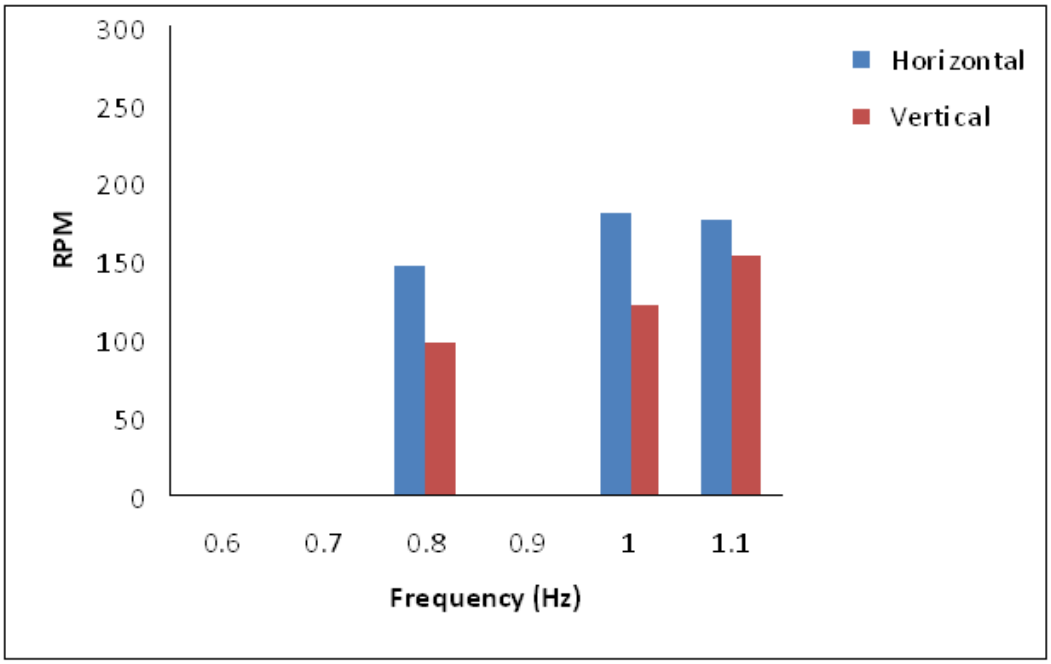

Fig. 12. RPM of the Savonius rotor for the two OWC models at different frequencies and D = 230 mm.

Figure 13

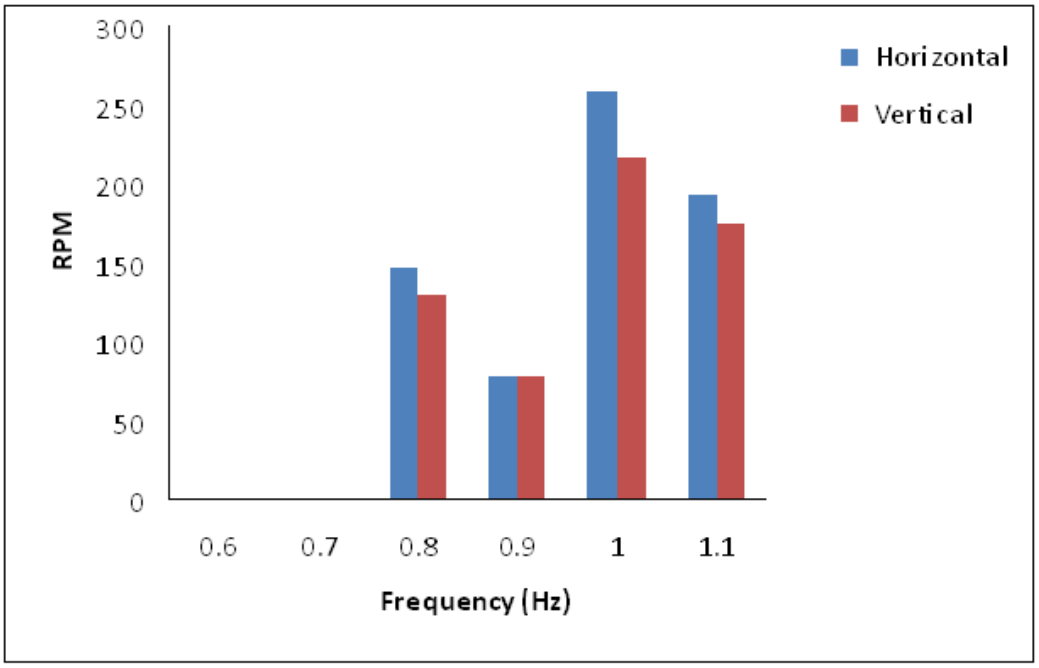

Fig. 13. RPM of the Savonius rotor for the two OWC models at different frequencies and D = 260 mm.

Figure 14

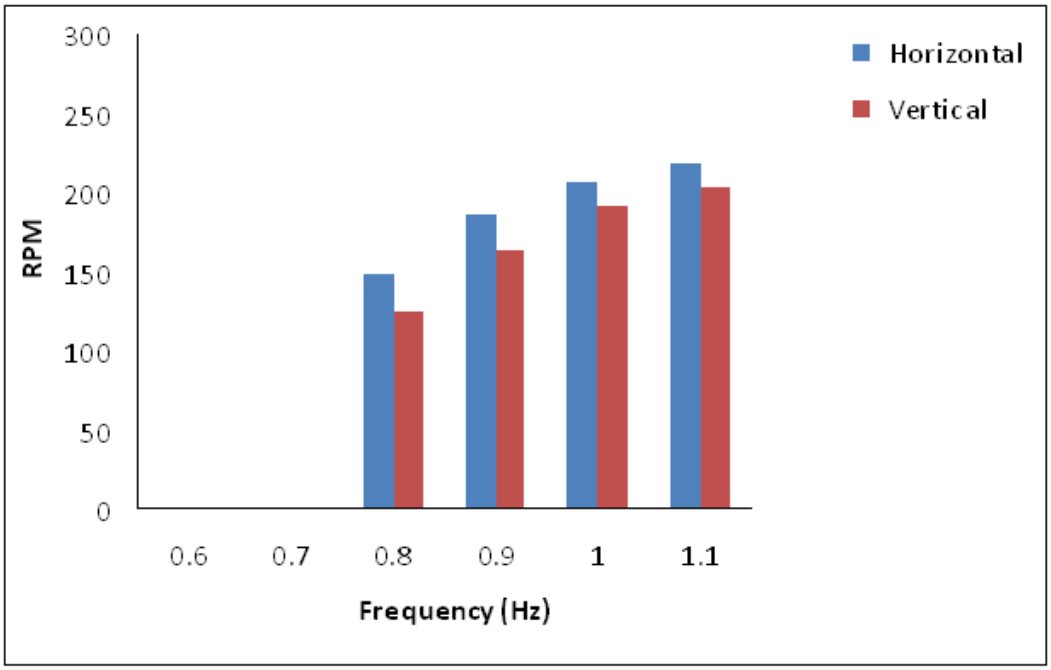

Fig. 14. RPM of the Savonius rotor for the two OWC models at different frequencies and D = 290 mm.

Table 1

Table 1. RPM of the Savonius rotor at different frequencies and depths

Frequency (f)	**D = 230 mm**		**D = 260 mm**		**D = 290 mm**	
(Hz)	**Horizontal**	**Vertical**	**Horizontal**	**Vertical**	**Horizontal**	**Vertical**
0.6	0	0	0	0	0	0
0.7	0	0	0	0	0	0
0.8	146.7	96.4	145.8	130.1	147.2	124.5
0.9	0	0	78.2	77.1	185.2	163.2
1	180.8	121.5	258.3	216.2	205.8	191.2
1.1	175.1	152.6	191.8	174.2	217.4	203.1